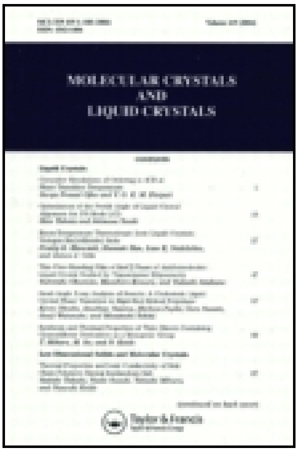

Molecular Crystals and Liquid Crystals
Publication details, including instructions for authors and subscription information:
http://www.tandfonline.com/loi/gmcl20

Effect of External Field on the Nematic to Isotropic Transition: An Entropic Sampling Study

Regina Jose [a], D. Jayasri [b], Surajit Dhara [a], K. P. N. Murthy [a] & V. S. S. Sastry [a]

[a] School of Physics, University of Hyderabad, Hyderabad, India

[b] Faculty of Mathematics and Physics, University of Ljubljana, Ljubljana, Slovenia

Version of record first published: 30 Jun 2011

To cite this article: Regina Jose, D. Jayasri, Surajit Dhara, K. P. N. Murthy & V. S. S. Sastry (2011): Effect of External Field on the Nematic to Isotropic Transition: An Entropic Sampling Study, Molecular Crystals and Liquid Crystals, 545:1, 168/[1392]-175/[1399]

To link to this article: http://dx.doi.org/10.1080/15421406.2011.571999

Mol. Cryst. Liq. Cryst., Vol. 545: pp. 168/[1392]–175/[1399], 2011
Copyright © Taylor & Francis Group, LLC
ISSN: 1542-1406 print/1563-5287 online
DOI: 10.1080/15421406.2011.571999

Effect of External Field on the Nematic to Isotropic Transition: An Entropic Sampling Study

REGINA JOSE,[1] D. JAYASRI,[2] SURAJIT DHARA,[1]
K. P. N. MURTHY,[1] AND V. S. S. SASTRY[1]

[1]School of Physics, University of Hyderabad, Hyderabad, India
[2]Faculty of Mathematics and Physics, University of Ljubljana, Ljubljana, Slovenia

Earlier experiments on the effect of an external field on the nematic-isotropic transition temperature indicate its linear increase with field in the low field regime, in contrast to a quadratic dependence at higher fields. This was explained phenomenologically as due to the effective suppression of longer wavelength order director modes at low fields. We investigate this effect by carrying out Monte Carlo simulation on a lattice model based on Lebwohl-Lasher potential. We achieve the necessary high temperature resolution (one part in 10^4) by performing an entropic sampling on the system, and our results support this phenomenological interpretation.

Keywords Entropic sampling; Monte Carlo methods; paranematic-nematic transition; Wang-Landau algorithm

1. Introduction

The anisotropic properties of the liquid crystalline phases, like nematics, arise from long range orientational order of the constituent anisotropic molecules while retaining fluid like flow behaviour. Coupling of external fields like electric field, to the resulting dielectric anisotropy of the medium leads to controllable molecular orientation. Its manifestation is for example seen as an observable shift in the nematic-isotropic (NI) transition temperature, as well as a weak orientational order in the high temperature isotropic phase (paranematic phase). It is known that this transition remains weakly first order for a material with positive dielectric anisotropy and it vanishes at a critical value of the applied field in the medium. The consequent changes in the (dis)order show up as observable variation in different physical properties, indicating new phases, and other field induced critical effects [1]. The effect of the applied electric field on the paranematic-nematic transition temperature (T_{PN}) was investigated experimentally in liquid crystals (LC) with both positive and negative dielectric anisotropies [2–7]. The nature of the transition is

---

Address correspondence to Regina Jose, School of Physics, University of Hyderabad, Hyderabad, 500046, India. Tel.: +91-40 23011033; Fax: +91-40 23010227; E-mail: reginajose.c@gmail.com

affected differently owing to the qualitative difference between the ordering directions induced by intermolecular interactions on one hand and the coupling of the molecules with the field on the other [8]. However, in both the cases it was experimentally shown that T_{PN} increases linearly for small applied fields ($\sim 10^7$ V/m) contrary to the expectation based on the Landau-de-Gennes energy considerations, which in fact predicts a quadratic dependence. The origin for this result (at low fields) is attributed to quenching of director fluctuation modes by the applied field leading to additional dependence on the field which turns out to be linear. Of course experimental detection of this subtle effect needs application of very low fields and hence require experimental facilities to measure rather very small shifts in temperature [5]. The enhancement in free energy, ΔF due to loss of entropy resulting from the quenching of long wavelength director modes was calculated phenomenologically by introducing two length scales: the electric coherence length $\xi \propto 1/|E_a|$ and the cut-off wave vector $q_c \propto 1/l$ (l is of the order of the molecular dimension). The enumeration of the modes in the presence of these two bounding cut-off wave vector amplitudes, needed to compute the decrease in the entropy at an applied field E_a, leads to [5]

$$\Delta F = \alpha|E_a| + \delta E_a^2 \tag{1}$$

Here $\delta << \alpha$, leading to prominent linear dependence on E_a in the low field regime. The experimentally observed linear shift in T_{PN}, in the field range up to 10^7 V/m, is within 0.2°C for medium with positive dielectric anisotropy and within 0.6°C for that with negative dielectric anisotropy.

In this context, the present work reports Monte Carlo simulation results on the variation of the paranematic-nematic transition temperature with applied field. The motivation is to see if the phenomenological interpretation of the experimental observation (in terms of quenching of certain director modes) is also borne out by carrying out simulations based on microscopic model. We used the well studied lattice-model (Lebwohl-Lasher) potential to simulate the results, augmented with a dielectric energy density contribution with the usual quadratic dependence on the field. The interest is to investigate if a linear dependence emerges from such a model at low enough fields. The challenge of achieving a high precision in the temperature variation during simulation was met by employing the more recent entropic sampling method (generally referred to as the non-Boltzmann sampling) [9], thereby achieving temperature resolution of the simulated results comparable to the experiments.

In section 2 we provide a brief introduction to the entropic sampling technique and details of simulation. Section 3 presents the results and discussion comparing them with experimental findings. Conclusions are presented in section 4.

2. (a) Entropic Sampling

In standard Monte Carlo simulations, based on given Hamiltonian models, a random walk is performed in the relevant configuration space seeking the required statistical distribution (the Boltzmann probability prescription) by the application of Metropolis algorithm [10]. The resulting set of microstates, after the equilibration, corresponds to the canonical ensemble appropriate to the set experimental conditions, primarily the temperature. This procedure, which is now termed as Boltzmann sampling, is to be repeated for each specific experimental condition and the equilibrium physical properties are averages over the respective ensemble of microstates. More recent sampling methods attempt at achieving very high resolution in temperature, while not needing to carry out separate simulation for each value. Besides, they also address with reasonable success certain non-trivial issues of quasi-ergodicity and critical slowing down, encountered for example near different phase transitions [11–15]. In such cases, a random walk is performed which is uniform with respect to the energy E of the system through a suitable algorithm. While the set of microstates collected during this energy-uniform walk are unphysical from experimental view point, they indeed contain all microstates relevant to the range of temperature of interest. Canonical ensembles appropriate to the desired temperatures are then extracted from the so-called entropic ensemble through reweighting procedure. We employ one such convenient algorithm [9], modified to suit LC systems [16] to construct those entropic ensembles. The crucial step in this procedure is the accurate estimate of the density of states $g(E)$ of the given system. Wang-Landau algorithm provides a learning procedure to compute $g(E)$. An energy-uniform ensemble is then readily obtained by performing a random walk, compensating for the bias in the configuration space due to inherent density distribution of states. The macroscopic value of any physical property, say O, in thermal equilibrium at temperature T ($\beta = 1/k_B T$), is then computed from the collection of microstates in the entropic ensemble $\{C_i\}$ by a reweighting procedure as

$$\langle O \rangle = \frac{\sum_{i=1}^{N} O(C_i) g(E(C_i)) \exp[-\beta E(C_i)]}{\sum_{i=1}^{N} g(E(C_i)) \exp[-\beta E(C_i)]} \tag{2}$$

(B) Model Potential and Simulation Details

In the lattice model used here, a cubic lattice (of length $L = 20$) is considered, imposing periodic boundary conditions to minimize the finite size effects. Each lattice site is occupied by a headless vector (typically representing a small group of uniaxial and apolar liquid crystal molecules), and the interactions among the lattice sites are restricted to only the nearest neighbours. Since the nematic-isotropic transition is primarily connected with the orientational degrees of freedom, one such lattice model (Lebwohl-Lasher) [17] permitting interactions based on the relative orientations of the molecules has been extensively used as it captures the essential features of the N-I transition remarkably well. We use this model for the present work, supplemented by the interaction term (with positive dielectric anisotropy) with the applied electric field. The total energy thus is expressed as

$$E = -\varepsilon \sum_{\langle ij \rangle} P_2(\cos(\theta_{ij})) - E_a^2 \sum_i P_2(\cos(\theta_i)) \tag{3}$$

where ε is the nearest neighbor positive coupling constant, θ_{ij} is the angle between unit vectors representing the local directors at i$^{\text{th}}$ and j$^{\text{th}}$ sites, θ_i is the angle between the local director at i$^{\text{th}}$ site and the field direction. ε sets the energy scale and the temperature T is specified in reduced units given by $T = k_B t/\varepsilon$, where t is the actual sample temperature. Due to the assumed positive dielectric anisotropy of the system, the applied field favours parallel alignment of the long axes with the field. After obtaining the density of states (DoS) with respect to E at a given field value as described above, several independent energy-uniform random walks were performed to collect a number of entropic ensembles each consisting of 3×10^7 microstates. This was found necessary to improve the statistical quality of the data to meet the experimental conditions. Computation of the different physical quantities, averaged over several canonical ensembles constructed under identical conditions yielded accuracies compatible with the experimental errors in the temperature measurement. Canonical ensembles so extracted have at least 7×10^5 microstates near the transition. Transition temperatures are determined from the peak position of specific heat C_V plotted as a function of temperature at each field value. The C_V values are computed from the energy fluctuations as

$$C_V = \frac{1}{K_B T^2}(\langle E^2 \rangle - \langle E \rangle^2) \tag{4}$$

T_{PN} values obtained from different canonical simulations (at a given T and E_a) are averaged so as to yield an error not exceeding 3×10^{-4}.

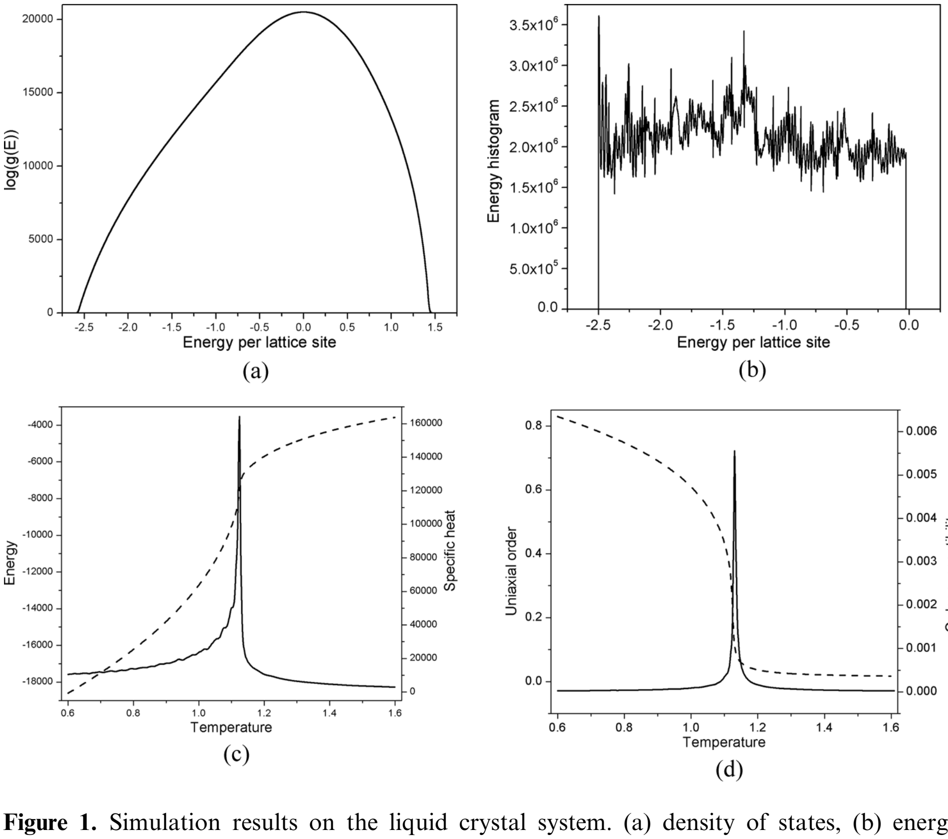

Figure 1. Simulation results on the liquid crystal system. (a) density of states, (b) energy histogram of the entropic ensemble, (c) temperature variation of equilibrium energy (dashed line) and specific heat (solid line), (d) orientational order (dashed line) and its susceptibility (solid line).

3. Results and Discussion

The results of Wang-Landau simulation without applied field are shown in Figure 1. Here, (a) and (b) show respectively, the density of states (DoS) with respect to energy, and the histogram recorded while collecting the microstates in the entropic ensemble. The temperature evolution of average energy, specific heat C_V, average orientational order and its susceptibility χ are shown in Figure 1(c) and Figure 1(d). For the temperature resolution achieved, the transition appears quite sharp as seen from the jump in the energy and in the order parameter near T_{PN}. This is also evident from the sharply peaked C_V and χ profiles.

$\Delta T_{PN} = T_{PN}(E_a) - T_{PN}(0)$ (i.e., shift in T_{PN}) determined from the position of the C_V peak is shown as a function of E_a in Figure 2. As may be seen, there are two distinct regions of variation of this shift with field. For low values of the field ($\lesssim 0.04$ in arbitrary units), the temperature shift is linear, tending to become quadratically dependent for higher values. As is shown in the inset of the figure, a linear fit seems to be appropriate in the low field region. The higher field regime fits very well to a polynomial in E_a of order 2, confirming the expected variation from the dielectric energy.

The variation of C_V with temperature for various fields is shown in Figure 3(a). It is observed that near and above $E_a \sim 0.15$, the C_V peak flattens considerably indicating softening of the transition in the presence of high enough fields. Of course this also makes the determination of the T_{PN} (at those high values) relatively more prone to errors. In fact in a positive dielectric liquid crystal medium, the trajectory of the transition with field is expected to end in a critical point. Our results are in agreement with reports on a system of 1000 particles wherein the critical value of E_a^2 was

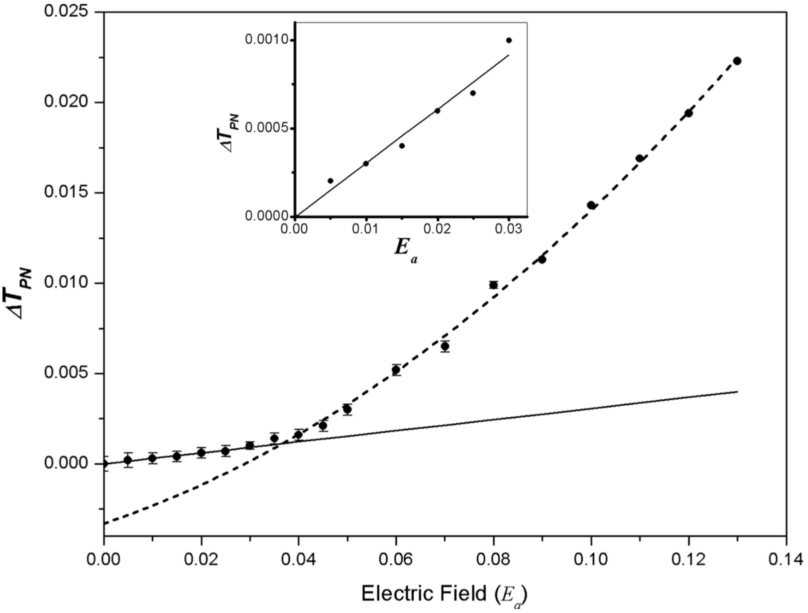

Figure 2. Variation of ΔT_{PN} with field (solid line is a linear fit and dashed line is a quadratic fit to the data in the low and high field regimes respectively). The inset focuses on the variation in the low field regime.

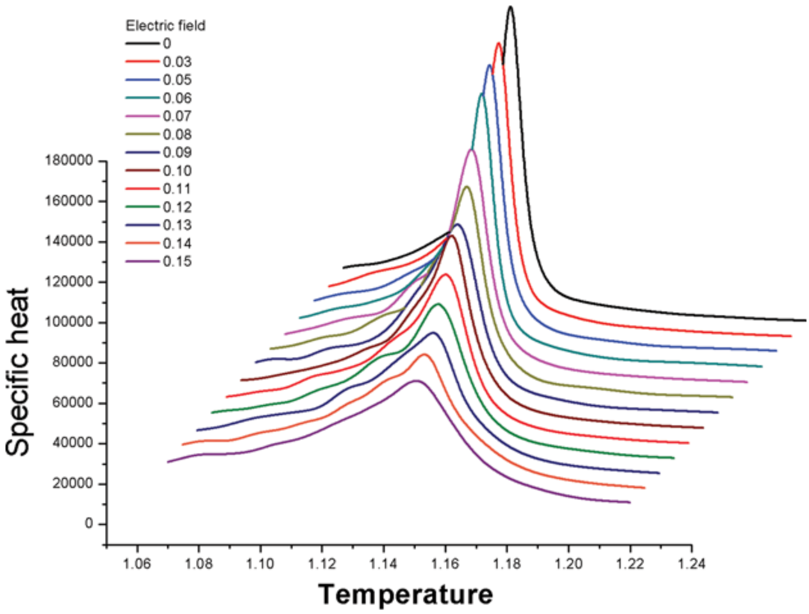

(a)

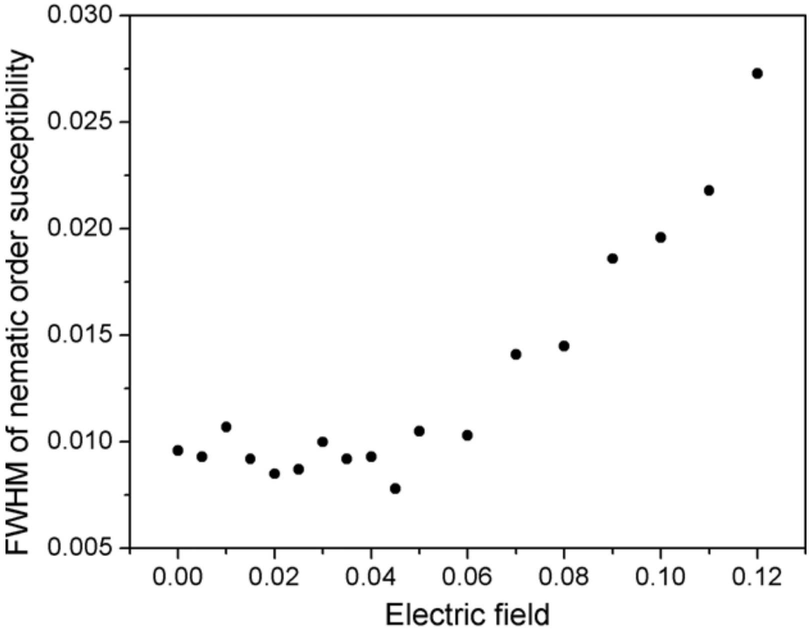

(b)

Figure 3. (a) Temperature variation of specific heat at various fields. (b) Variation of the widths of nematic susceptibility (FWHM) with applied field. (Figure appears in color online.)

reported to be well below 0.2 [6]. The softening of the transition with increase of applied field is also seen from the variation of the width i.e., full width at half maximum (FWHM) of the nematic susceptibility (computed from reweighting

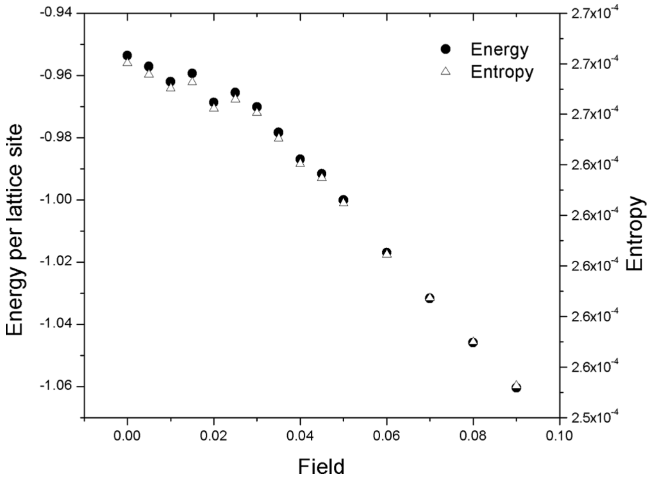

Figure 4. Energy per lattice site (solid circles) and the corresponding representative entropy (open triangles) versus applied field at $T = 1.1239$ (just below $T_{PN}(E_a = 0)$).

results of a single entropic ensemble) and is shown in Figure 3(b). This width remains almost constant in the lower field regime (consistent with linear temperature shift) and increases for the higher field values. This seems to indicate that the thermally driven fluctuations in the order near the PN transition are effectively quenched at the lower values of E_a.

The field dependence of energy at a temperature just below the PN transition is shown in Figure 4 (solid circles). The corresponding values of entropy computed from the DoS data i.e., $\log(g(E))$ is also shown in this figure (open triangles). It may be noted that the values of the entropy shown are representative being accurate to within an additive constant, and are obtained by appropriate normalization of DoS over the chosen energy range. It is remarkable that despite the quadratic dependence of the energy on the applied field introduced through the Hamiltonian, the macroscopic energy and consequently the associated entropy, show striking linear behaviour at low fields conforming both the experimental observations, as well as lending support to the phenomenological view point of partial quenching of director modes over a length scale determined by the interplay of the applied field strength and the elastic constant.

3. Conclusion

We determine the shift in the paranematic-nematic transition temperature due to the application of an electric field in a liquid crystal system with positive dielectric anisotropy. We used recent Monte Carlo simulation methods which permits high accuracy and resolution in computing the phase transition temperatures. Our results agree with the experimental observation of the linear temperature shift at the very low fields. Further, the observed variation of energy and the representative entropy, with applied field, also exhibit a linear behavior in the corresponding field regime thus lending support to the phenomenological interpretation of the observed data in terms of partial quenching of director modes in the presence of applied fields.

Acknowledgment

The authors acknowledge Centre for Modeling Simulation and Design, University of Hyderabad for providing computational facilities. RJ thanks CSIR, New Delhi for the award of Research Fellowship.

References

[1] Dunmur, D. A., & Palffy-Muhoray, P. (1988). *J. Phys. Chem.*, *92*, 1406.
[2] Helfrich, W. (1970). *Phys. Rev. Lett.*, *24*, 5.
[3] Nicarsto, A. J., & Keyes, P. H. (1984). *Phys. Rev., A*, *30*, 6.
[4] Lelidis, I., & Durand, G. (1993). *Phys. Rev. E*, *48*, 5.
[5] Surajit Dhara, & Madhusudana, N. V. (2004). *Europhysics Lett.*, *67*, 411, and references therein.
[6] (a) Luckhurst, G. R., Simpson, P., & Zannoni, C. (1981). *Chem. Phys. Lett.*, *78*, 3; (b) Luckhurst, G. R., & Simpson, P. (1983). *Chem. Phys. Lett.*, *95*, 2.
[7] (a) Turalski, W., Miniewicz, A., & Mitus, A. C. (1997). *Adv. Mat. Opt. Elec.*, *7*, 71; (b) Turalski, W. Mitus., Miniewicz, A. C., & Miniewicz, A. (1997). *Pure Appl. Opt.*, *6*, 589.
[8] Gramsbergen, E. F., Longa, L., & De Jeu, W. H. (1986). *Physics Reports*, *135*, 195.
[9] Wang, F., & Landau, D. P. (2001). *Phys. Rev. Lett.*, *86*, 2050; *Phys. Rev. E.*, *64*, 056101.
[10] Metropolis, N., Rosenbluth, A. W., Rosenbluth, M. N., Teller, A. H., & Teller, E. (1953). *J. Chem. Phys.*, *21*, 1087.
[11] Torrie, G., & Valleau, J. P. (1974). *Chem. Phys. Lett.*, *28*, 578.
[12] Ferrenberg, A. M., & Swendsen, R. H. (1989). *Phys. Rev. Lett.*, *63*, 1195.
[13] Berg, B. A., & Neuhaus, T. (1992). *Phys. Rev. Lett.*, *68*, 9.
[14] Lee, J. (1993). *Phys. Rev. Lett.*, *71*, 211.
[15] Venu, K., Sastry, V. S. S., & Murthy, K. P. N. (2002). *Europhys Lett.*, *58*, 646.
[16] Jayasri, D., Sastry, V. S. S., & Murthy, K. P. N. (2005). *Phys. Rev. E.*, *48*, 3822.
[17] Lebwohl, P. A., & Lasher, G. (1972). *Phys. Rev. A*, *6*, 426.